American Journal of Applied Mathematics
2025; 13(6): 438-451
http://www.sciencepublishinggroup.com/j/ajam
doi: 10.11648/j.ajam.20251306.16

Unsteady Hydro-magnetic Stagnation Flow and Heat and Mass Transfer Past A Stretching Surface in the Presence Chemical Reaction Embedded in a Porous Medium

Deva Kanta Phukan*

Demow College (Sivasagar), Dibrugarh, India

Email address:
drdevakanta63@gmail.com (Deva Kanta Phukan)
*Corresponding author

To cite this article:
Deva Kanta Phukan. (2025). Unsteady Hydro-magnetic Stagnation Flow and Heat and Mass Transfer Past A Stretching Surface in the Presence Chemical Reaction Embedded in a Porous Medium. *American Journal of Applied Mathematics, 13*(6), 438-451. https://doi.org/10.11648/j.ajam.20251306.16

Received: 9 September 2025 ; **Accepted:** 04 October 2025 ; **Published:** 19 December 2025

Abstract: A theoretical analysis is made on the unsteady stagnation point flow of a conducting fluid over a flat stretching surface in the presence of magnetic field with chemically reactive species concentration and mass diffusion under Soret and Dufour effects. The governing partial differential equations of continuity, momentum, energy and concentration have been converted to self-similar unsteady equations by using similarity transformations and solved numerically by the Runge-Kutta algorithm with Newton iteration in double precisions along with the shooting method across the boundary layer for the whole transient domain from the initial state to the final steady state flow. The effects of existing flow parameters viz Soret number, Dufour number, chemical reaction parameter, Darcy number and magnetic parameter are shown graphically for the dimensionless velocity, temperature and concentration of the conducting fluid.The velocity of the conducting fluid is seen to decrease across the boundary layer with increasing the magnetic parameter, Prandtl number, Schmidt number and chemical reaction parameter; and the velocity profiles are seen to increase with increasing the thermal Grashof number, mass Grashof number, Soret number, stretching parameter and Dufour number. The temperature is seen to decrease with increasing the Prandtl number, Soret number, stretching parameter, and the same temperature are found to increase with increasing Dufor number and Chemical reaction parameter across the boundary layer.In the same way, the concentration is seen to reduce with increasing Schmidt number, Dufour number, stretching parameter,chemical reaction parameter and but concentration increases with increasing Soret number. Further more, numerical results for the skin friction, Nusselt number and Sherwood number are tabulated for various flow parameters.It is clearly observed from the result that a smooth transition of flow of conducting fluid is seen from unsteady stage to the final steady stage. Skin friction decreases with the increasing magnetic parameter, Schmidt number, Prandtl number and chemical reaction parameter and same skin friction increases with the increasing Soret numbe, Dufour number, thermal and concentration buoyancy parameters, Darcy number, stretching parameter and dimensionless time. Nusselt number is seen to increase with increasing the value of Soret number, Prandtl number, stretching parameter, dimensionless time and the same Nusselt number decreases with increasing the value of Dufour number, chemical reaction parameter and Schmidt number. Sherwood number is seen to decrease with increasing the value of Soret number, Dufour number, Prandtl number and dimensionless time and is seen to increase with increasing Chemical reaction parameter, stretching parameter and Schmidt number. The results obtained in this investigation are seen good agreement with earlier published results in some particular cases.

Keywords: Stagnation Flow, Magnetic Field, Soret and Dufour Number, Chemical Reaction, Porous Media, Conducting Fluid, Heat and Mass Transfer

1. Introduction

In recent years of studies of last few decades, the problems focusing on the stagnation -point flow towards a stretching surface have been reported in the literature by researchers due to its industrial and engineering applications such as extrusion, paper production, insulating materials, glass drawing and continuous casting. In the same way, the problems of heat and mass transfer flows of conducting fluid under the influence of magnetic field have been attracted the attention of a number of researchers because of its possible applications in different branches of science and technology. Further more, a renewed interest has been observed among the researchers in studying particularly Magneto-hydrodynamics flow associated with heat and mass transfer problems in different mathematical modeling.Numerous publications have been appeared in the leading journal in and and abroad. It is observed that the effect of an applied magnetic field on fluid flow, mass and heat transfer are useful for cooling processes in the presence of an electrolytic bath.In some metallurgical processes, such as drawing, annealing and those that involve the cooling of continuous strips of filament by drawing tinning of copper wires etc, the properties in quiescent fluid of the final product depend to a great extent on the rate of cooling. The rate of cooling can be controlled by drawing such strips in an electrically conducting fluid subject to a magnetic field, and the final product of desired characteristic can be achieved.

The simultaneous heat and mass transfer phenomenon from different geometries embedded in porous media has many engineering and geophysical applications such as geothermal reservoirs, drying of porous solids, thermal insulation, enhanced oil recovery, packed-bed catalytic reactors, cooling of nuclear reactors, and underground energy transport. The two dimensional stagnation point flow was initiated by Hiemenz [1] who discovered that the equations governing the flow can be transformed into third-order ordinary differential by using similarity transformation. Sakiadis [2] first, studied the boundary layer flow over a stretching surface and later on, Crane [3] extended this problem for both linear and exponentially stretching sheet. The steady two dimensional stagnation -point flow of a viscous fluid towards a stretching sheet was studied by Chiam [4].The flow of mass diffusion of a chemical species with first order and higher order reactions over a linearly stretching surface was investigated by Anderson et al. [5]. Anjalidevi and Kandasamy [6] studied the steady laminar flow along a semi-infinite horizontal plate in the presence of a species concentration and chemical reaction. Muthucumaraswamy [7] investigated the chemical reaction effect of a on a moving isothermal vertical infinitely long surface with suction. An extensive amount of studies presented by several researchers in ([8-12]).Abbas et al. [13] studied stagnation point flow of a hydro-magnetic viscous fluid over a stretching/shrinking with generalized slip condition in the presence of homogeneous-heterogeneous reaction. A numerical approach to boundary layer stagnation point flow past a stretching/ shrinking sheet was discussed by Dash et al. [14]. Seth et al. [15] investigated the MHD stagnation point flow and heat transfer past a non-isothermal shrinking/stretching sheet in porous medium with heat sink or source effect. Veerkrishna et al. [16] discussed the heat and mass transfer on MHD free convective flow over an infinite non-conducting vertical porous plate. ShankarGoud [17] discussed the stagnation point flow through a porous medium towards a stretching surface in the presence oh heat generation. Feleke et al. [18] presented stagnation flow of a magnetite ferro fluid past a convectively heated permeable stretching /shrinking sheet in a Darcy- Forchheimer porous medium. Makinde et al. [19] analized Dual solutions of MHD flow and heat and mass transfer on surface stretching problem. Vishalaskhi et al. [20] investigated on Hiemenz stagnation point flow with computational modeling in variety of boundary conditions. Reddy [21] forwarded a presentation on Outlining the impact modeling on MHD cassion fluid flow past a stretching sheet in a porous medium with radiation. Recently, several problems having relevance to the field of present problem were performed by several researches through their contribution heat and mass transfer on immiscible fluid flow through porous matrix, unsteady MHD rotating mixed convective flow considering Joule heating, thermal radiation, Hall current and radiation absorption, and heat and mass transfer by MHD flow near the stagnation point over a stretching surface in a porous medium in ([22-24]).

The present paper is an extension work of Nayak et al. [12], which is investigated in different mathematical model and as a result momentum equation and boundary conditions appear in different form from Nayak et al. [12]. The purpose of the present paper is to study the simultaneous heat and mass transfer of an unsteady hydro-magnetic stagnation flow of conducting fluid over a stretching surface embedded in a saturated porous medium with chemically reactive species. There exists new flow parameters in this investigation. In absence of some existing flow parameters the results correspond to some earlier published work.

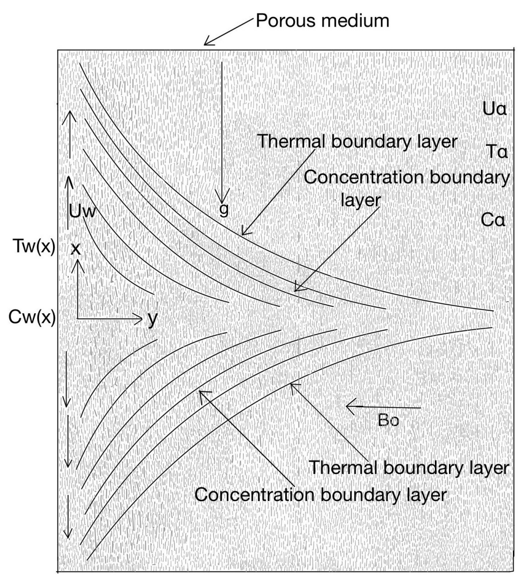

Figure 1. Sketch of stagnation flow model.

2. Mathematical Formulation of the Problem

We consider the problem of an unsteady two dimensional viscous, incompressible, laminar stagnation flow through a porous medium on to a vertical flat stretching surface in the presence of transverse magnetic field with chemically reactive species concentration . The x-axis is taken along the stretching direction of the plate with stretching rate $U_e(x) = ax$ where $a > 0$, and y-axis is normal to the surface of the plate.. A magnetic field of uniform strength B_0 is applied in the negative direction of the y-axis and the gravity acts in the negative direction of x-axis Since the sheet is considered as non-conducting and the effects of radiation, the viscous dissipation and the Hall effects are neglected. The magnetic Reynolds number of the flow is taken to be small enough so that the induced magnetic field is almost negligible and the Joule heating is also neglected, while the magnetic effects, Darcy number, Soret, Dufour and chemical reaction parameter effects are examined. The density variation and the buoyancy effect are taken into consideration which could be adopted the Boussinesq approximations for both the temperature and concentration gradient in the momentum equation. Further more, the physical properties, i.e., the viscosity, heat capacity, the thermal diffusivity, and the mass diffusivity of the fluid remain invariant throughout the field.

Initially, the plate and the fluid are at the same temperature T_∞ in a stationary condition with concentration level C_∞. At time $t > 0$ the fluid starts moving with the stretching rate U_e and its temperature and concentration at the plate raised to T_w and C_w respectively. Under these assumption, the governing boundary layer equations of mass, momentum, energy and diffusion under Boussinesq approximation can be written as follows

$$\frac{\partial u}{\partial x} + \frac{\partial v}{\partial y} = 0, \tag{1}$$

$$\frac{\partial u}{\partial t} + u\frac{\partial u}{\partial x} + v\frac{\partial v}{\partial y} = \nu\frac{\partial^2 u}{\partial y^2} + U_\infty\frac{dU_\infty}{dx} + g\beta_t(T - T_\infty) + g\beta_c(C - C_\infty) + \frac{\nu}{K}(u - U) - \frac{\sigma B_0^2}{\rho}(u - U), \tag{2}$$

$$\frac{\partial T}{\partial t} + u\frac{\partial T}{\partial x} + v\frac{\partial T}{\partial y} = \alpha\frac{\partial^2 T}{\partial y^2} + \frac{D_\epsilon k_T}{C_s C_p}\frac{\partial^2 C}{\partial y^2}, \tag{3}$$

$$\frac{\partial C}{\partial t} + u\frac{\partial C}{\partial x} + v\frac{\partial C}{\partial y} = D_\epsilon\frac{\partial^2 C}{\partial y^2} - K_1(C_w - C_\infty) + \frac{D_\epsilon k_T}{T_m}\frac{\partial^2 T}{\partial y^2}. \tag{4}$$

The initial and boundary conditions of equations (1)-(4) are

$$\left\{\begin{array}{l} t < 0: \ u = 0, \ v = 0, \ T = T_\infty, \ C = C_\infty, \\ t \geq 0, u = u_w = U_e(x) = ax, \ v = 0, \ T = T_w = T_w + bx, \\ C = C_w = C_\infty + bx \\ u = U_a = cx, \ T = T_\infty, \ C = C_\infty, \end{array}\right\}. \tag{5}$$

where u and v are the velocity components along the x-axis and y -axis respectively; c and a are the positive constant that represent the characteristics intensity and the free stream strength respectively, U the flow velocity T and C are the temperature and concentration variables, ν is the kinematic viscosity, ρ is the density, σ is the electrical conductivity, α is the thermal diffusivity, D_e is the mass diffusivity, g is the acceleration due to gravity, C_p the specific heat at constant pressure, K_T, C_s and T_m are the thermal diffusion ratio, concentration susceptibility and fluid mean temperature respectively; β_t is the thermal expansion co-efficient, β_c is the concentration expansion co-efficient, K is the permeability of the porous medium, K_1 is the dimensional chemical reaction parameter a and b are constant.

Introducing the flowing change of variables as Rashad and El- Kabeir[11]

$$\left\{\begin{array}{l} \tau = at, \quad \eta = \sqrt{\frac{a}{\nu}}\,\xi y \\ \quad \xi = 1 - exp(-\tau), \quad \psi = \sqrt{a\nu}\,x\,\xi f(\xi,\tau), \\ \theta = \frac{T - T_\infty}{T_w - T_\infty}, \quad \phi = \frac{C - C_\infty}{C_w - C_\infty}, \end{array}\right\} \tag{6}$$

where ψ is the stream function which is defined as

$$u = \frac{\partial \psi}{\partial y} \quad and \quad v = -\frac{\partial \psi}{\partial x}. \tag{7}$$

The equation of continuity (1) is identically satisfied which can be easily verified. It is convenient for us to select the time scale ξ so that the region of time integration $0 < \tau < \infty$ occurs $0 < \xi < 1$. Using (8) and (9), the equation (2), (3) and (4) converts to

$$f''' + \frac{1}{2}(1-\xi)\,\eta\, f'' + \xi\, ff'' + \xi(S^2 + M + \frac{1}{D_a}S) \quad + \xi(G\theta + N\phi) - \xi(\frac{1}{D_a} + M + f')f' = \xi(1-\xi)\frac{\partial f'}{\partial \xi} \tag{8}$$

$$\frac{1}{P_r}\theta'' + \frac{1}{2}(1-\xi)\eta\theta' + \xi(f\theta' - f'\theta) + D_f\phi'' = \xi(1-\xi)\frac{\partial \theta'}{\partial \xi}, \tag{9}$$

$$\frac{1}{S_c}\phi'' + \frac{1}{2}(1-\xi)\eta\phi' + \xi f\phi' - \xi(f'\phi) + \gamma\phi) + S_r\theta'' = \xi(1-\xi)\frac{\partial \phi'}{\partial \xi}. \tag{10}$$

.

where prime denotes differentiation with respect to η, $D_a = \frac{kc}{\nu}$ is the Darcy number, $M = \frac{\sigma B_0^2}{\rho}$ is the magnetic parameter, $S = \frac{a}{c}$ is the stretching parameter, $G = \frac{g\beta_T(T_w - T_\infty)}{cu_w}$ is the temperature buoyancy parameter(thermal Grashof number), $N = \frac{g\beta_C(C_w - C_\infty)}{cu_w}$ is concentration buoyancy parameter (mass Grashof number), $P_r = \frac{\nu}{\alpha}$ is the Prandtl number, $D_f = \frac{D_e K_T (C_w - C_\infty)}{C_s C_p \gamma (T_w - T_\infty)}$ is the Dufour number, $S_r = \frac{D_e K_T (T_w - T_\infty)}{T_m \gamma (C_w - C_\infty)}$ is the Soret number, $S_c = \frac{\nu}{D}$ is the Schmidt number and $\gamma = \frac{K_1}{a}$ is the dimensionless parameter of chemical reaction parameter for porous medium.

The transformed boundary conditions are

$$\left.\begin{aligned} f(\xi,0) = 0, f'(\xi,0) = 1, \theta(\xi,0) = 1, \phi(\xi,0) = 1 \\ f'(\xi,\infty) = S, \theta(\xi,\infty) = 0, \phi(\xi,\infty) = 0 \end{aligned}\right\}. \tag{11}$$

It is clearly observed and may be noted that for $M = D_f = S_r = S = 0$, Equations (8)-(11) correspond to the equations as obtained by Rashad and El-Kabeir [11].

3. Numerical Solution of the Problem

The Equations (8)-(10) together with boundary conditions (11) are the system of ordinary differential equations with a set of constraints at the boundary and can be easily solved by standard numerical method. The solution procedure for the entire time domain $0 \le \xi \le 1$ is discussed in the succeeding section.

3.1. Solution at Initial Stage (State) When $\xi = 0$

When time scale $\xi = 0$, i.e. for initial unsteady flow, it corresponds to $\tau = 0$, the equation (8)-(10) converts to

$$f''' + \frac{1}{2}\eta f'' = 0, \tag{12}$$

$$\frac{1}{P_r}\theta'' + \frac{1}{2}\eta\theta' + D_f\phi'' = 0 \tag{13}$$

and

$$\frac{1}{S_c}\phi'' + \frac{1}{2}\eta\phi' - \gamma\phi + S_r\theta'' = 0, \tag{14}$$

subject to the boundary conditions

$$\left.\begin{aligned} f(0) = 0, \quad f'(0) = 1, \quad \theta(0) = 1, \quad \phi(0) = 1 \\ f'(\infty) = S, \quad \theta(\infty) = 0, \quad \phi(\infty) = 0 \end{aligned}\right\}. \tag{15}$$

Equations (13) and (14) for $D_f = S_r = 0$, correspond to the same as those presented by Rashad and El-Kabeir [11]. One may also refer that equation (15) for $S = 0$ corresponds to the same as those presented by Nayak et al. [12].

3.2. Solution for Steady State When $\xi = 1$, i.e. Final Steady Flow

When time scale $\xi = 1$, corresponding to $\tau \to \infty$, equations(8)-(10) becomes

$$f''' + ff'' + S^2 + MS + \frac{1}{D_a}S + G\theta + N\phi - (\frac{1}{D_a} + M + f')f' = 0, \tag{16}$$

$$\frac{1}{P_r}\theta'' + f\theta' - f'\theta + D_f\phi'' = 0 \tag{17}$$

and

$$\frac{1}{S_c}\phi'' + f\phi' - (\gamma + f')\phi + S_r\theta'' = 0 \tag{18}$$

subject to the boundary conditions

$$\left.\begin{aligned} f(1,0) = 0, \; f'(1,0) = 1, \; \theta(1,0) = 1, \; \phi(1,0) = 1 \\ f'(1,\infty) = S, \; \theta(1,\infty) = 0, \; \phi(1,\infty) = 0 \end{aligned}\right\}. \tag{19}$$

It is observed from equation (16) that for $M = 0$ coresponds to the equations obtained by Rashad and El-Kabeir [11] and for $S = 0$ the equation (19) corresponds to the same as obtained by Nayak et al. [12].

3.3. Solution for Small ξ or τ

The solutions of equation (8)-(10) subject to the boundary conditions (11), which are valid for the region $\xi \le 1$ equivalent to the small time $\tau << 1$ solution, can be expressed as

$$f(\xi,\eta) = f_0(\eta) + \xi f_1(\eta) + \xi^2 f_2(\eta) + - - -, \tag{20}$$

$$\theta(\xi,\eta) = \theta_0(\eta) + \xi\theta_1(\eta) + \xi^2\theta_2(\eta) + --, \tag{21}$$

$$\phi(\xi,\eta) = \phi_0(\eta) + \xi\phi_1(\eta) + \xi^2\phi_2(\eta) + --, \tag{22}$$

where

$$f_0''' + \frac{1}{2}\eta f_0'' = 0, \tag{23}$$

$$\frac{1}{P_r}\theta_0'' + \frac{1}{2}\eta\theta_0' + D_f\phi_0'' = 0 \tag{24}$$

and

$$\frac{1}{S_c}\phi_0'' + \frac{1}{2}\eta\phi_0' - \gamma\phi_0 + S_r\theta_0'' = 0, \tag{25}$$

subject to the boundary conditions

$$\left.\begin{aligned} f_0(0) = 0, \; f_0'(0) = 1, \; \theta_0(0) = 1, \; \phi_0(0) = 1 \\ f_0'(\infty) = S, \; \theta_0(\infty) = 0, \; \phi_0(\infty) = 0 \end{aligned}\right\}, \tag{26}$$

$$f_1''' + \frac{1}{2}(f_1'' - f_0'')\eta + S^2 + G\theta_0 + N\phi_0 - (\frac{1}{D_a} + M)(f_0' - S) - f_0^2 = 0, \quad (27)$$

$$\frac{1}{P_r}\theta_1'' + \frac{1}{2}\eta(\theta_1' - \theta_0') + f_0\theta_0' - f_0'\theta_0 - \theta_1 + D_f\phi_1'' = 0, \quad (28)$$

$$\frac{1}{S_c}\phi_1'' + \frac{1}{2}\eta(\phi_1' - \phi_0') + f_0\phi_0' - f_0'\phi_0 - \phi_1 - \gamma\phi_1 + S_r\theta_1'' = 0, \quad (29)$$

subject to the boundary conditions

$$\left.\begin{aligned} f_1(0) = 0,\ f_1'(0) = 0,\ \theta_1(0) = 0,\ \phi_1(0) = 0 \\ f_1'(\infty) = 0,\ \theta_1(\infty) = 0,\ \phi_1(\infty) = 0 \end{aligned}\right\}. \quad (30)$$

and

$$f_2''' + \frac{1}{2}(f_2'' - f_1'')\eta + f_0f_1'' + f_1f_0'' - 2f_0'f_1' + G\theta_1 + N\phi_1 - \frac{1}{D_a}f_1' - Mf_1' - 2f_2' = 0, \quad (31)$$

$$\frac{1}{P_r}\theta_2'' + \frac{1}{2}\eta(\theta_2' - \theta_1') + f_0\theta_1' + f_1\theta_0' - f_0'\theta_1 - \theta_0f_1' - 2\theta_2 + \theta_1 + D_f\phi_2'' = 0, \quad (32)$$

$$\frac{1}{S_c}\phi_2'' + \frac{1}{2}\eta(\phi_2' - \phi_1') + f_0\phi_1' + f_1\phi_0' - f_0'\phi_1 - \phi_0f_1' - 2\phi_2 + \phi_1 - \gamma\phi_2 + S_r\theta_2'' = 0, \quad (33)$$

subject to the boundary conditions

$$\left.\begin{aligned} f_2(0) = 0,\ f_2'(0) = 0,\ \theta_2(0) = 0,\ \phi_2(0) = 0 \\ f_2'(\infty) = 0,\ \theta_2(\infty) = 0,\ \phi_2(\infty) = 0 \end{aligned}\right\}. \quad (34)$$

The aforesaid system of ordinary differential equations with respective boundary conditions of this problem are at different regimes.So we need to solve the problem step by step to obtain the solutions in the entire time domain $0 \le \xi \le 1$. For the solution of the initial state $\xi = 0$ and final state $\xi = 1$, we have solve equations (12)-(15) and (16)-(19) respectively. For the solution in the time domain $0 < \xi < 1$, we need to solve equations (27)-(29) and (31)-(33) subject to the respective boundary condition (30) and (34). But the leading order perturbed equations (23)-(25) with the boundary condition (30) are the same as the equations of unsteady solution at the initial state $\xi = 0$.

Equations (23)-(25), (27)-(29) and (31)-(33) subject to the respective boundary conditions (26), (30) and (34) are integrated using Runge-Kutta method accompanied Newton iteration in double precisions along with the shooting technique by selecting suitable guess values for each and every existing parameter so as to converse the numerical programe for the aforesaid non linear coupled differential equations (23)-(25), (27)-(29) and (31)-(33) subject to the respective boundary conditions (26),(30) and (34). The numerical results so obtained for $f_0, f_1, f_2, f_o', f_1', f_2', \theta_0, \theta_1, \theta_2$, ϕ_0, ϕ_1 and ϕ_2, are substituted in to equations (20)-(22), we get the appropriate typical profile of the non-dimensional velocity, temperature and concentration across the boundary layer for time domain $0 < \xi < 1$. The dimensionless flow field, temperature and concentration are analyzed in detail for different values of magnetic parameter, Prandtl number, Schmidt number, temperature buoyancy parameter , concentration buoyancy parameter, surface stretching parameter, chemical reaction parameter, Soret and Dufour parameters and dimensionless time in the forthcoming section.

4. Results and Discursion

A representative set of graphical results is plotted to show the influence of various exiting flow parameters on the velocity f', the temperature θ and concentration field ϕ through graphs (Figures 2-12) from initial state ($\xi = 0$) to the final steady state ($\xi = 1$) . Figures 2(a), (b) and (c) show the velocity, temperature and concentration profiles respectively; for various non-dimensional time ξ with $P_r = 0.71$, $S_c = 0.6$, $N = 1$,$G = 2$ $D_a = 5$, $S_r = 1$, $M = 2$, $D_f = 0.1$, $S = 0.1$ and $\gamma = 0.8$. The velocity is seen to increase gradually from ($\xi = 0$) to ($\xi = 1$) as shown in Figure 2(a) but the temperature and concentration profiles are seen to as shown in Figure 2(b) and Figure 2(c) respectively for the same domain of ξ. and these results agree with the earlier results Rashad and El-Kabeir [11].

The effect of Darcy number D_a on the dimensionless velocity along the stretching surface is displayed in Figure 3(a). A higher Darcy number implies a more permeable medium, allowing fluid to flow more easily with less resistance and leads to increase fluid velocity. Hence the velocity profiles f' increases with increasing the Darcy number D_a for fixed $P_r = 0.71$, $S_c = 0.6$, $N = 1$, $G = 2$, $S_r = 1$, $M = 2$, $D_f = 0.1$, $S = 0.1$ and $\gamma = 0.8$.

The surface stretching parameter S effects on dimensionless velocity f' , temperature θ and concentration ϕ of the conducting fluid across the boundary layer are shown in Figure 3 (b), Figure 3(c) and Figure 4(a) respectively for fixed $P_r = 0.71$, $S_c = 0.6$, $N = 1$, $G = 2$, $S_r = 1$, $M = 2$, $D_f = 0.1$, $D_a = 5$ and $\gamma = 0.8$. Since the parameter$S$ stands for the ratio of free stream strength compared to the stretching intensity and so the effects of stretching parameter S are to increase the dimensionless free stream velocity with increasing S as shown in Figure 3 (b). while reverse effect of stretching parameter S is observed on the temperature and concentration of the conducting fluid as shown in Figure 3(c) and Figure 4(a). That is, temperature and concentration of the fluid fall down due to increasing the surface stretching parameter S.

In Figure 4(b) shows the typical profiles for the dimensionless velocity f' for various magnetic parameter M

for fixed $P_r = 0.71$, $S_c = 0.6$, $N = 1$, $G = 2$, $S_r = 1$, $S = 0.1$, $D_f = 0.1$, $D_a = 5$ and $\gamma = 0.8$. The effect of magnetic parameter M on the motion of the conducting fluid reduces the velocity f' across the boundary layer due to the existence of retarding Lorentz force. But the influences of magnetic parameter M i.e. Lorentz force on the dimensionless temperature θ and concentration ϕ are not visible in this investigation. Figure 4(c) shows the temperature profiles θ for various Schmidt number S_c and concentration profiles ϕ for various Prandtl number P_r is shown in Figure 5(a). The effect of Schmidt number S_c is to increase the temperature profiles first and then start to decrease across the boundary layer. The same effect of Prandtl P_r is observed in concentration profile as shown in Figure 5(a).

The Dufour effects on the dimensionless velocity f', temperature θ and concentration ϕ are shown in Figure 5(b), Figure 5(c) and Figure 6(a) respectively for fixed $P_r = 0.71$, $S_c = 0.6$, $N = 1$, $G = 2$, $S_r = 1$, $S = 0.1$, $M = 2$, $D_a = 5$ and $\gamma = 0.8$. It is observed from Figure 5(b) and Figure 5(c) that the effects of Dufour number D_f are to increase the dimensionless velocity f' and temperature θ of the conducting fluid across the boundary layer but concentration ϕ as shown in Figure 6(a) is seen to decrease with increasing values of Dufour number D_f. The insight physical phenomenon is due to the presence of Dufour term in the energy equation which plays a significant role in enhancing the flow velocity and the ability to increase the thermal energy in the boundary layer. Figure 6(b), Figure 6(c) and Figure 7(a) demonstrate the distribution of velocity f', temperature θ and concentration ϕ respectively for different Soret parameter S_r for fixed $P_r = 0.71$, $S_c = 0.6$, $N = 1$, $G = 2$, $D_f = 0.1$, $S = 0.1$, $M = 2$, $D_a = 5$ and $\gamma = 0.8$. The soret number appears in the concentration equation measures the contribution of temperature gradient to mass flux across the boundary layer. Hence the influence of soret number are to increase the velocity and concentration of the fluid as shown in Figure 6(b) and 7(a) respectively. But the effect of Soret parameter S_r is to reduce temperature across the boundary layer as shown in Figure 6(c). Figure 7(b), Figure (c) and Figure 8(a) show the distribution of velocity f', temperature θ and concentration ϕ for various chemical parameter γ respectively for fixed $P_r = 0.71$, $S_c = 0.6$, $N = 1$, $G = 2$, $D_f = 0.1$, $S = 0.1$, $M = 2$, $D_a = 5$ and $S_r = 1$. It can be clearly seen from the above Figures that the velocity and concentration distribution decrease with the increase in the chemical reaction parameter γ (see Figure 7(b) and Figure 8(a)) which implies that the concentration boundary layer becomes thinner, and at the same time, the concentration diffusion species decrease. But the temperature increases due to the reduction in mass diffusion (see Figure 7 (c)) and which results the decrease in the velocity.

Figure 8(b) represents the dimensionless concentration distribution ϕ across the boundary layer for different Schmidt number S_c for fixed $\gamma = 0.8$, $P_r = 0.71$, $N = 1$, $G = 2$, $D_f = 0.1$, $S = 0.1$, $M = 2$, $D_a = 5$ and $S_r = 1$. Since the Schmidt number S_c measures the ratio of momentum diffusivity to mass diffusivity, and a higher S_c implies that momentum diffuses faster than the substance, resulting in a thinner concentration boundary layer. So the concentration of the fluid decreases for lower value of S_c in the solutal boundary layer.

Figure 8(c) represents the dimensionless temperature distribution θ across the boundary layer for different Prandtl number P_r for fixed $\gamma = 0.8$, $S_c = 0.6$, $N = 1$, $G = 2$, $D_f = 0.1$, $S = 0.1$, $M = 2$, $D_a = 5$ and $S_r = 1$. Since the Prandtl number P_r measures the ratio of momentum diffusivity to thermal diffusivity, and a higher P_r implies lower thermal diffusivity which means heat diffuses slower. Consequently, the temperature distribution within the fluid tends to be more concentrated near the stretching surface, which leads to decrease in over all temperature.

It can be clear from Figure 9(a) and Figure 9(b) that the effects of both thermal buoyancy parameter G and concentration buoyancy parameter N on the dimensionless velocity f' of the conducting fluid are seen to increase across the boundary layer respectively for fixed $\gamma = 0.8$, $P_r = 0.71$, $S_c = 0.6$, $D_f = 0.1$, $S = 0.1$, $M = 2$, $D_a = 5$ and $S_r = 1$. This is due to the physical point of view as the higher thermal buoyancy parameter G indicates a greater temperature variation, which causes stronger buoyancy forces due to density differences and so the fluid velocity increases across the boundary layer.That is, it induces more flow along the vertical plate/sheet which causes the higher velocity of the fluid, i.e. assisting the flow in upward direction. Furthermore, concentration buoyancy parameter N relates to density variations caused by concentration gradients within the fluid and results in increased fluid velocity. This phenomenon occurred insight the flow velocity at the expense of both the temperature and concentration of the conducting fluid across the boundary layer.

Figure 9(c) show the distribution of velocity f' for various Schmidt number S_c for fixed $P_r = 0.71$, $\gamma = 0.8$, $N = 1$, $G = 2$, $D_f = 0.1$, $S = 0.1$, $M = 2$, $D_a = 5$ and $S_r = 1$. A higher Schmidt number S_c leads to a lower mass diffusivity relative to momentum diffusivity, which tends to reduce velocity. This is due to the fluid's ability to transport mass is diminished and impacting the overall flow characteristics. A combined effects of Prandtl number and Schmidt number on the velocity profiles is shown in Figure 10(a) . It is seen that velocity decreases for both Prandtl number and Schmidt number because both describe the relative importance of momentum diffusion compared to other transport phenomena.

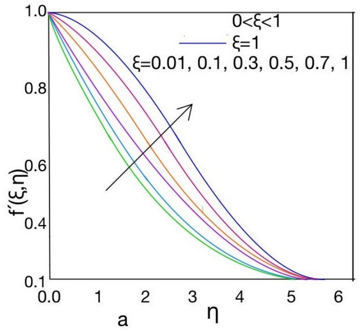

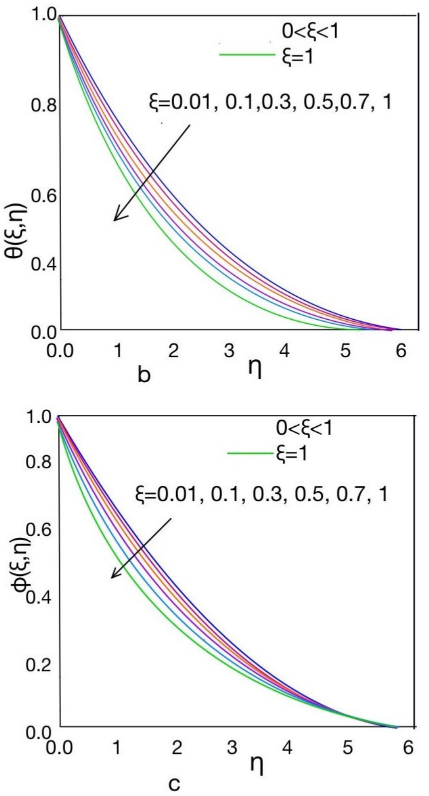

Figure 2. *a) Velocity distribution for different ξ. b) Temperature distribution for different ξ.c) Concentration distribution for different ξ.*

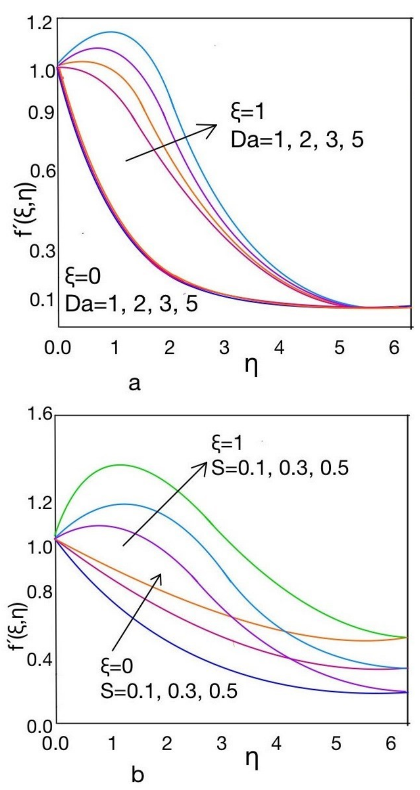

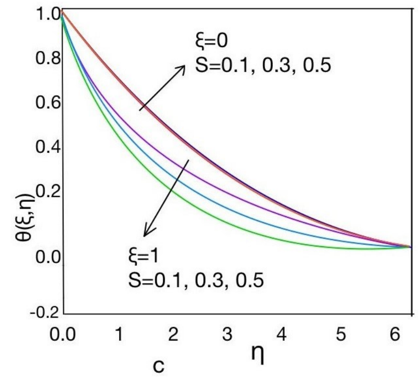

Figure 3. *a) Velocity distribution for different Darcy parameter D_a. b) Velocity distribution for different stretching parameter S.c) Temperature distribution for different stretching parameter S. c) Concentration distribution for different stretching parameter S.*

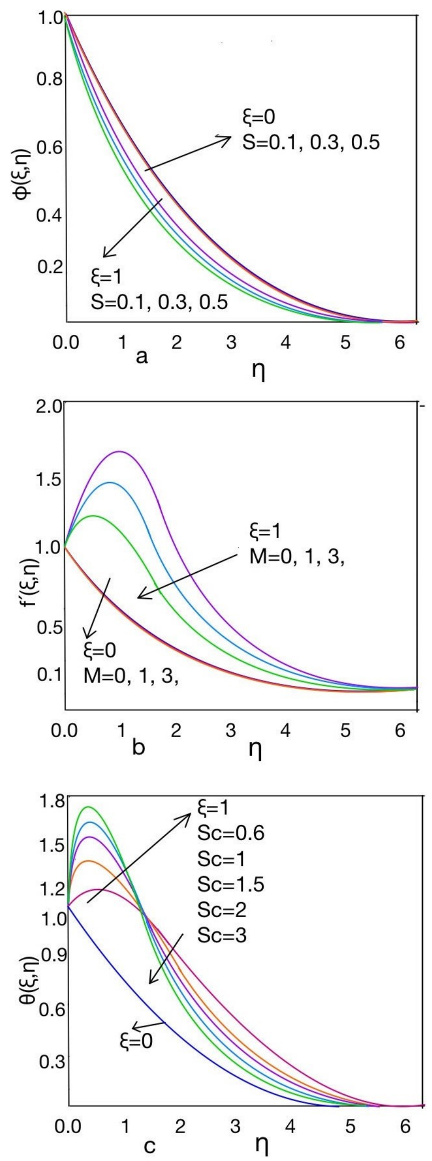

Figure 4. *a) Concentration distribution for different stretching parameter S.b) Velocity distribution for different magnetic parameter M. c) Temperature distribution for different Schmidt number S_c.*

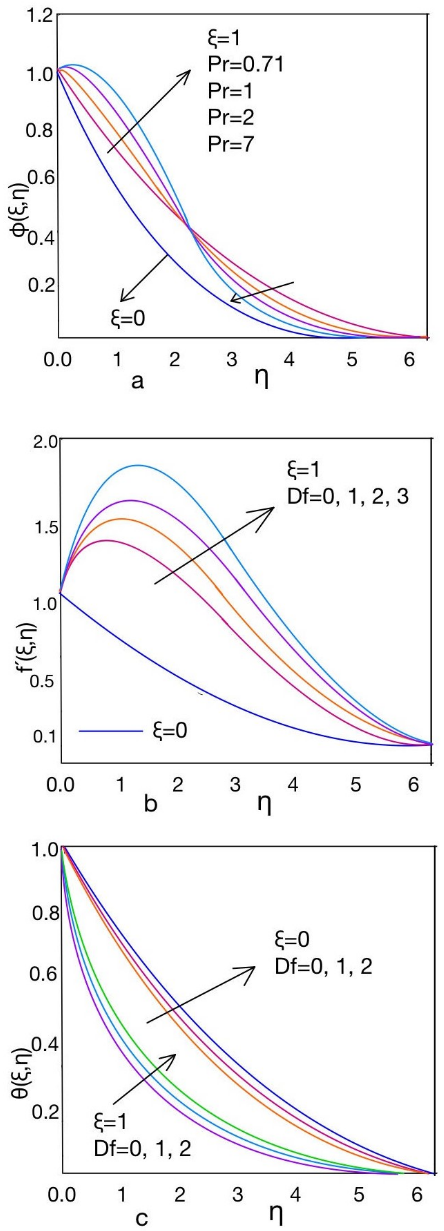

Figure 5. *a) Concentration distribution for different Prandtl number P_r.b) Velocity distribution for different Dufour parameter D_f.c)Temperature distribution for different Dufour parameter D_f.*

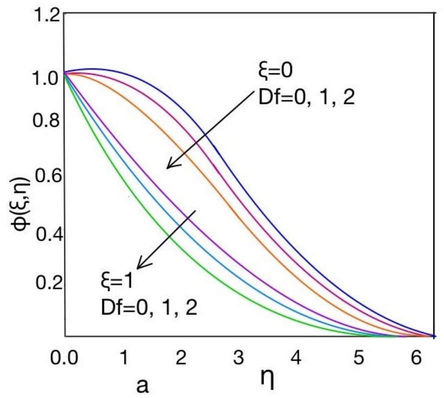

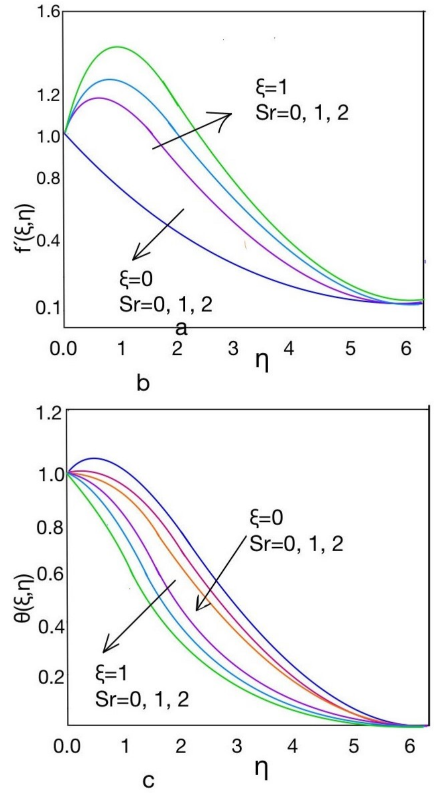

Figure 6. *a) Concentration distribution for different Dufour parameter D_f.b) Velocity distribution for different Soret parameter S_r. c) Temperature distribution for different Soret parameter S_r.*

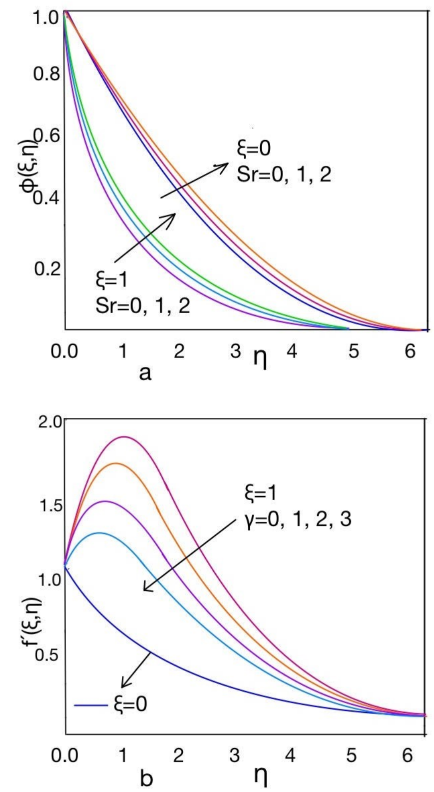

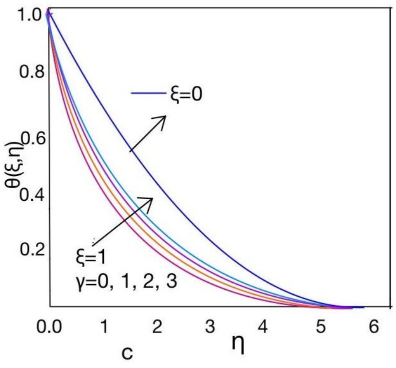

Figure 7. *a) Concentration distribution for different Soret parameter S_r.b) Velocity distribution for different chemical reaction parameter γ.c)Temperature distribution for different chemical reaction parameter γ.*

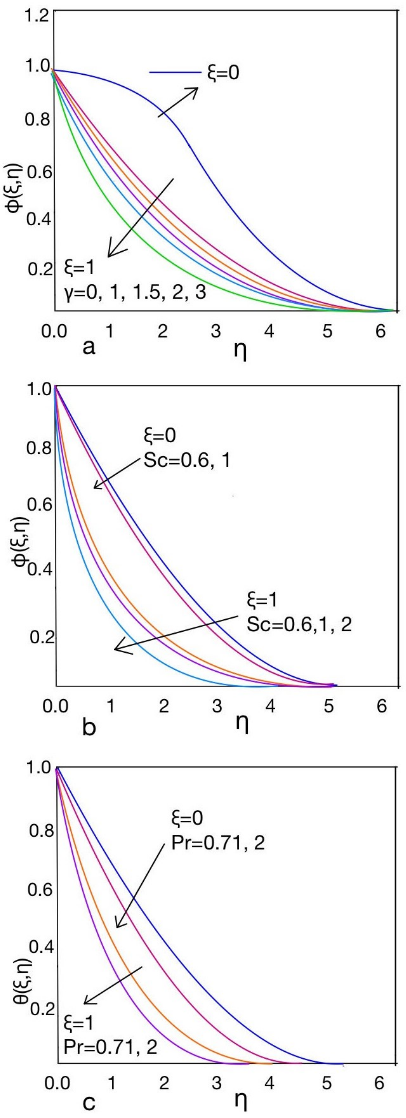

Figure 8. *a) a) Concentration profiles for different chemical reaction parameter γ.b) Concentration profiles for different Schmidt number S_c c) Temperature profiles for different Prandtl number P_r.*

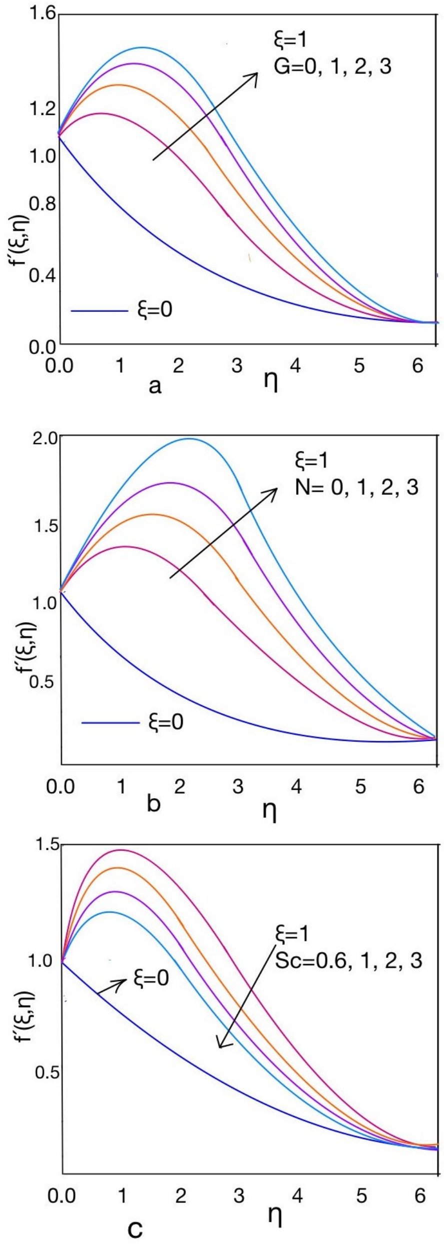

Figure 9. *a) Velocity profiles for different thermal buoyancy parameter G. b) Velocity profiles for different concentration buoyancy parameter N.c) Velocity profiles for different Schmidt number S_c.*

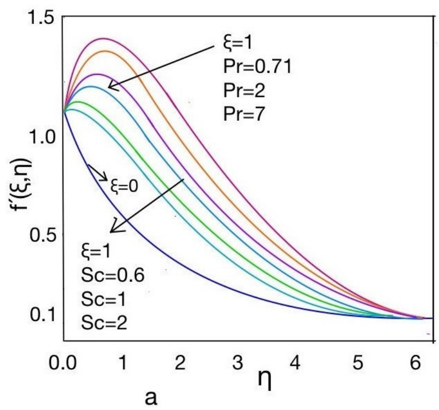

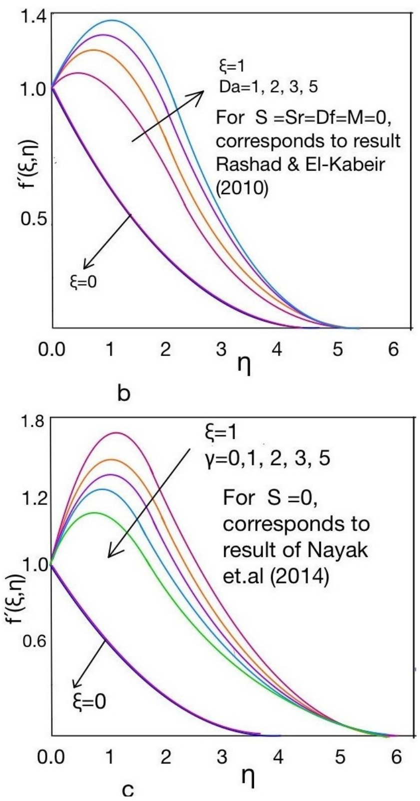

Figure 10. *a) Combined velocity distribution for different Prandtl number P_r and Schmidt number S_c. b) Velocity profiles for different Darcy number D_a for $S = S_r = D_f = M = 0$. c) Velocity distribution for different chemical reaction parameter γ for $S = 0$.*

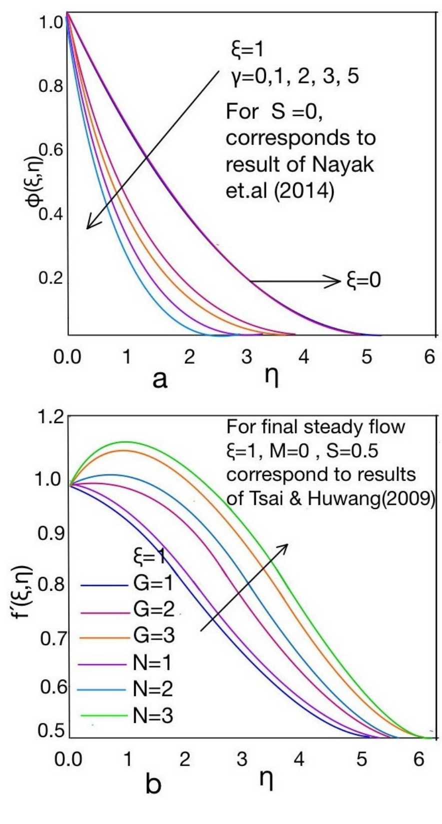

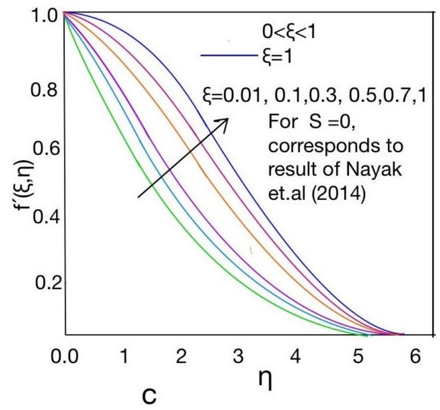

Figure 11. *a) Concentration distribution for different chemical reaction parameter γ for $S = 0$. b) Concentration profiles for different ξ. b) Velocity distribution for different G and N for $M = 0$, $S = 0.5$ for final steady flow $\xi = 1$.c) Velocity distribution for different ξ for $S = 0$. Velocity distribution for different D_a.*

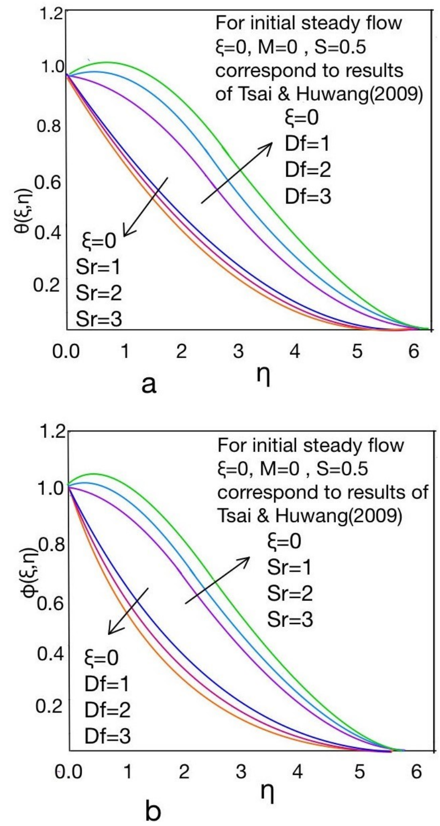

Figure 12. *a)Temperature distribution for different Dufour parameter D_f and Soret parameter S_r for initial state $\xi = 0$. b) Concentration distribution for different Soret parameter S_r and Dufour parameter D_f for initial state $\xi = 0$.*

5. Validation of Numerical Procedure and Results

A direct numerical solution of the governing equation non-linear coupled ordinary differential equation cannot be obtained and also these set of differential equations (23)-(25), (27)-(29) and (31)-(33) subject to the respective boundary conditions (26), (30) and (34) cannot be solved analytically also. Because there are always missing some initial conditions in prescribed boundary conditions. The shooting method is a standard one which is suitable method that converts boundary value problem to initial value problem and then can be possible to solve by fourth order Runge-Kutta algorithm with newton iteration in double precision with a systematic guessing $f_0''(0)$, $\theta_0'(0)$, $\phi_0'(0)$,$f_1''(0)$, $\theta_1'(0)$, $\phi_1'(0)$, $f_2''(0)$, $\theta_2'(0)$, and $\phi_2'(0)$ due to not prescribing these values at the initial point of integration. The error arises during simulation at the infinity because domain under consideration is not bounded but the computational domain is finite.In the investigation, the boundary conditions at the end of boundary layer is fixed to 7 and less than 7 after adjustment of physical parameters of the problem .

The validation of the result may be referred the Darcy number effect on the dimensionless velocity profiles from ($\xi = 0$) to ($\xi = 1$) in Figure 10(b) for $S = S_r = D_f = M = 0$ which is excellent agreement with the results obtained by Rashad and El-Kabeir [11]. The chemical reaction effects on velocity and concentration from ($\xi = 0$) to ($\xi = 1$) are presented in absence of stretching parameter i.e. $S = 0$ in Figure 10(c) and Figure 11(a) respectively which excellently agree with the results obtained by Nayak et al. [12].
we may also present the final steady flow for $\xi = 1$ in absence of magnetic filed in Figure 11(b) to show the effects of both thermal Grashof number and mass Grashof number in absence of magnetic field $M = 0$ which are good agreement with the results presented by Tsai and Huang [10]. The velocity profiles presented in Figure 11(c) in absence of stretching parameter i.e. $S = 0$ in the domain $0 < \xi \leq 1$ correspond to the result of Nayak et al. [12]. Furthermore, we may refer the effects of soret and Dufour number on the temperature and concentration of the fluid in absence of magnetic field i.e. $M = 0$, in Figs 12(a) and Figure 12(b) are in good agreement with the results presented by Tsai and Huang [10].

6. Skin Friction, Nusselt Number and Sherwood Number

The dimensionless skin-friction coefficient , the Nusselt number and the Sherwood number are important physical parameters for this type of boundary layer flow of the conducting fluid where the local skin-friction coefficient $C_f = \tau_w/\rho U_e^2(x)/2$ with the skin friction $\tau_w = \mu(\partial u/\partial y)_{y=0}$, the local Nusselt number $Nu_x = q_w x/\kappa(T_w - T_\infty)$ with heat transfer from the flat stretching surface $q_w = -\kappa(\partial T/\partial y)_{y=0}$ and the local Sherwood number $Sh_x = m_w x/D(C_w - C_\infty)$ with the local mass transfer coefficient $m_w = -D_e(\partial C/\partial y)_{y=0}$ where ρ, μ and κ are the density, dynamic viscosity and thermal conductivity of the conducting fluid respectively. The aforesaid quantities those have physical interest in this problem may be expressed in terms of(non-dimensional quantities) transformation variables as defined below respectively

$$Skin\ friction\ C_f = (\frac{\partial u}{\partial \eta})_{\eta=0} = 2Re_x^{-\frac{1}{2}}\xi^{-\frac{1}{2}}f''(\xi,0), \tag{35}$$

$$Nusselt\ number, Nu_x = (\frac{\partial \theta}{\partial \eta})_{\eta=0} = -Re_x^{-\frac{1}{2}}\xi^{-\frac{1}{2}}\theta'(\xi,0), \tag{36}$$

$$Sherwood\ number, Sh_x = (\frac{\partial \phi}{\partial \eta})_{\eta=0} = -Re_x^{-\frac{1}{2}}\xi^{-\frac{1}{2}}\phi'(\xi,0). \tag{37}$$

Table 1 show the variation of co-efficient of skin friction, dimensionless rate of heat transfer and rate of mass transfer for different magnetic parameter M. It is seen that increasing the magnetic parameter M strongly reduces the value of skin-friction at time $\xi = 0.1$ for fixed other parameters. No effects are seen apparently on rate of heat transfer and rate of mass transfer . The effects of thermal buoyancy parameter G and concentration buoyancy parameter N on skin-friction, Nusselt number and Sherwood number are shown in Table 2 and Table 3 respectively. Both parameters reduce the value of the co-efficient of skin friction. The Prandtl number P_r effects are seen to make reduce the skin-friction and rate of mass transfer i.e. Sherwood number; and to make enhance the rate of heat transfer in Table 4. It is obvious that Skin- friction and Sherwood number decrease with increase of Prandtl number P_r and Nusselt number increases with increase of P_r . Table 5 shows the effect of Schmidt number S_c on skin-friction, Nusselt number and Sherwood number at time $\xi = 0.1$ for fixed other parameters. It is clear from Table 5 that skin-friction and Nusselt number are seen to decrease with increase of S_c where as Sherwood number increases with increase of S_c . It is also seen from Table 6 that skin friction increases with increase of Darcy number D_a where as no effects are observed on Nusselt number and Sherwood number. The effects of Soret number S_r on skin friction, Nusselt number and Sherwood number are shown in Table 7 where skin-friction and Nusselt number are seen to increase with increase of S_r while reverse effect is seen in case of Sherwood number. That is, rate of mass transfer decreases with increase of S_r in the presence of magnetic field. The influences of Dufour number D_f on skin friction, Nusselt number and Sherwood number is shown in Table 8. It is seen from Table 8 that skin friction increases with increase of Dufour number D_f but with the increasing values of D_f both rate of heat transfer and rate of mass transfer are seen to decrease at time $\xi = 0.1$ for fixed other parameters. The influences of chemical reaction parameter γ on skin friction, Nusselt number and Sherwood number are shown in Table 9. From table 9, it can be clear that due to presence of chemical reaction parameter γ ; skin friction and Nusselt number decrease with increase of γ and Sherwood number increase with increase of γ. Effect of surface stretching parameter S on skin friction, Nusselt number and Sherwood number is shown in Table 10 in the presence of magnetic field where skin friction, Nusselt number and Sherwood number are observed to increase with increasing values of S at time $\xi = 0.1$ for fixed other parameters. Moreover, with increasing the values of time $\xi = 0.1$, the skin-friction, Nusselt number and Sherwood number are seen to increase from Table 10 in the presence of chemical reaction and magnetic field.

Table 1. *Effects of magnetic parameter M on skin friction, Nusselt number, and Sherwood number for $P_r = 0.71$, $S_c = 0.6$, $G = 1$, $N = 1$, $D_a = 0.1$, $S_r = 1$, $D_f = 0.5$, $S = 0.2$, $\gamma = 0.5$ and $\xi = 0.1$.*

M	$f''(0)$	$-\theta'(0)$	$-\phi'(0)$
0	-0.674529	0.579396	0.713774
1	-0.742990	0.579396	0.713774
2	-0.802745	0.579396	0.713774
3	-0.862500	0.579396	0.713774
5	-0.982010	0.579396	0.713774
10	-1.280784	0.579396	0.713774

Table 2. *Effects of concentration buoyancy parameter N on skin friction, Nusselt number, and Sherwood number for $P_r = 0.71$, $S_c = 0.6$, $G = 1$, $D_a = 0.1$, $S_r = 1$, $M = 2$, $D_f = 0.5$, $S = 0.2$, $\gamma = 0.5$ and $\xi = 0.1$.*

N	$f''(0)$	$-\theta'(0)$	$-\phi'(0)$
1	-0.991680	0.579396	0.713774
2	-0.933230	0.579396	0.713774
5	-0.757880	0.579396	0.713774
7	-0.640980	0.579396	0.713774

Table 3. *Effects of Prandtl number P_r on skin friction, Nusselt number, and Sherwood number for $G = 1$, $S_c = 0.6$, $N = 1$, $D_a = 0.1$, $S_r = 1$, $M = 2$, $D_f = 0.5$, $S = 0.2$, $\gamma = 0.5$, and $\xi = 0.1$.*

P_r	$f''(0)$	$-\theta'(0)$	$-\phi'(0)$
0.71	-0.991680	0.579396	0.713774
1	-0.992433	0.625603	0.681791
7	-1.009912	2.235355	0.275946

Table 4. *Effects of Schmidt number S_c on skin friction, Nusselt number, and Sherwood number for $G = 1$, $P_r = 0.71$, $N = 1$, $D_a = 0.1$, $S_r = 1$, $M = 2$, $D_f = 0.5$, $S = 0.2$, $\gamma = 0.5$ and $\xi = 0.1$.*

S_c	$f''(0)$	$-\theta'(0)$	$-\phi'(0)$
0.6	-0.991680	0.579396	0.713774
1	-0.993595	0.537308	0.835766
3	-0.999246	0.374969	1.307146
5	-1.001990	0.253449	1.669077

Table 5. *Effects of Darcy number D_a on skin friction, Nusselt number, and Sherwood number for $P_r = 0.71$, $S_c = 0.6$, $G = 1$, $N = 1$, $M = 2$, $S_r = 1$, $D_f = 0.5$, $S = 0.2$, $\gamma = 0.5$ and $\xi = 0.1$.*

D_a	$f''(0)$	$-\theta'(0)$	$-\phi'(0)$
0.1	-0.991778	0.579396	0.713774
0.2	-0.693003	0.579396	0.713774
0.3	-0.588104	0.579396	0.713774
0.4	-0.539473	0.579396	0.713774
0.6	-0.490841	0.579396	0.713774
0.8	-0.594219	0.579396	0.713774
1	-0.453984	0.579396	0.713774
2	-0.424107	0.579396	0.713774

Table 6. *Effects of Soret number S_r on skin friction, Nusselt number, and Sherwood number for $P_r = 0.71$, $S_c = 0.6$, $G = 1$, $N = 1$, $M = 2$, $D_a = 0.1$, $D_f = 0.5$, $S = 0.2$, $\gamma = 0.5$ and $\xi = 0.1$.*

S_r	$f''(0)$	$-\theta'(0)$	$-\phi'(0)$
1	-0.991680	0.579396	0.713774
3	-0.988057	0.633988	0.555623
5	-0.984578	0.687623	0.400234
10	-0.976556	0.816999	0.0223653

Table 7. *Effects of Dufour number D_f on skin friction, Nusselt number, and Sherwood number for $P_r = 0.71$, $S_c = 0.6$, $G = 1$, $N = 1$, $M = 2$, $D_a = 0.1$, $S_r = 1$, $S = 0.2$, $\gamma = 0.5$ and $\xi = 0.1$.*

D_f	$f''(0)$	$-\theta'(0)$	$-\phi'(0)$
0.5	-0.991680	0.579396	0.713774
1	-0.989789	0.506165	0.712891
2	-0.986166	0.361734	0.711064
5	-0.976530	0.054662	0.705280

Table 8. *Effects of chemical reaction parameter γ on skin friction, Nusselt number, and Sherwood number for $P_r = 0.71$, $S_c = 0.6$, $G = 1$, $N = 1$, $M = 2$, $D_a = 0.1$, $S_r = 1$, $S = 0.2$, $D_f = 0.5$ and $\xi = 0.1$.*

γ	$f''(0)$	$-\theta'(0)$	$-\phi'(0)$
0.5	-0.991778	0.579396	0.713774
0.8	-1.000561	0.546709	0.8008281
1	-1.005177	0.514692	0.864901
2	-1.020332	0.479564	0.9983021
3	-1.029037	0.435006	1.131286
5	-1.039162	0.231057	1.720710

Table 9. *Effects of surface stretching parameter S on skin friction, Nusselt number, and Sherwood number for $P_r = 0.71$, $S_c = 0.6$, $G = 1$, $N = 1$, $M = 2$, $D_a = 0.1$, $S_r = 1$, $\gamma = 0.5$, $D_f = 0.5$ and $\xi = 0.1$.*

S	$f''(0)$	$-\theta'(0)$	$-\phi'(0)$
0.2	-0.991680	0.579396	0.713774
0.5	-0.586172	0.583924	0.714956
0.8	-0.167410	0.588452	0.716038
1.0	0.119128	0.591471	0.716926

Table 10. Effects of ξ on skin friction, Nusselt number, and Sherwood number for $P_r = 0.71$, $S_c = 0.6$, $G = 1$, $N = 1$, $M = 2$, $D_a = 0.1$, $S_r = 1$, $\gamma = 0.5$, $D_f = 0.5$ and $S = 0.2$.

ξ	$f''(0)$	$-\theta'(0)$	$-\phi'(0)$
0.1	−0.991680	0.579396	0.713774
0.2	−1.447777	−0.610636	0.722106
0.4	−2.359971	−0.673117	−0.738771
0.6	−3.272165	−0.735597	−0.755435
0.8	−4.184359	−0.798077	−0.772099

7. Concluding Remarks

This worked studied the unsteady Hydro-magnetic stagnation flow and heat and mass transfer through a porous medium onto a stretching surface in the presence of chemical reaction. The governing partial differential equations were transformed into non-dimensional coupled non-linear ordinary differential equations with appropriate boundary conditions and are solved by integrating using Runge-Kutta method accompanied with the shooting technique .

The dimensionless velocity profiles are observed to reduce across the boundary layer with increasing the magnetic parameter, Prandtl number, Schmidt number and chemical reaction parameter; and the velocity profiles are seen to increase with increasing the thermal Grashof number, mass Grashof number, Soret number, stretching parameter and Dufour number across the boundary layer.

The dimensionless temperature profiles are observed to decrease with increasing the Prandtl number, Soret number, stretching parameter, and the temperature are observed to increase with increasing Dufor number and Chemical reaction parameter across the boundary layer.

The dimensionless concentration profiles of the conducting fluid is reduced with increasing Schmidt number, Dufour number, stretching parameter, chemical reaction parameter and but concentration increases with increasing Soret number.

The dimensionless velocity profiles is seen in good agreement for thermal Grashof number G and mass Grashof number N in absence of magnetic field $M = 0$ with earlier published result.

The dimensionless velocity profiles excellently agree with previous published work in absence of stretching parameter i.e. $S = 0$ in the domain $0 < \xi \leq 1$.

The dimensionless temperature profiles and Concentration are seen in good agreement for Soret number S_r and Dufour number D_f in absence of magnetic field $M = 0$ and dimensionless time $\xi =$ with earlier published result.

Skin friction decreases with the increasing magnetic parameter, Schmidt number, Prandtl number and chemical reaction parameter and same skin friction increases with the increasing Soret numbe, Dufour number, thermal and concentration buoyancy parameters, Darcy number, stretching parameter and dimensionless time.

Nusselt number and Sherwood number are observed to remain same with increasing magnetic parameter M, i.e. No effects are also seen on Nusselt number and Sherwood number in the presence of magnetic field in this investigation with increasing the parameters G, N, D_a.

Nusselt number is seen to increase with increasing the value of Soret number, Prandtl number, stretching parameter, dimensionless time and the same Nusselt number decreases with increasing the value of Dufour number, chemical reaction parameter and Schmidt number.

Sherwood number is observed to decrease with increasing the value of Soret number, Dufour number, Prandtl number and dimensionless time and same Sherwood number increases with increasing chemical reaction parameter, stretching parameter and Schmidt number.

Acknowledgments

The author is very much grateful to Reviewer and Editor for their constructive and valuable suggestions for improving this paper during preparation.

Author Contributions

Deva Kanta Phukan is the sole author. The author read and approved the final manuscript.

Conflicts of Interest

The author declares no conflicts of interest.

References

[1] Hiemenz, K. (1911). Die Grenzschicht an einem in den gleichformigen Fluessigkeitsstrom eingetauchten geraden Kreiszylinder. Dinglers Polytechnisches Journal, 321, 321-410.

[2] Sakiadis, B. C. (1961). Boundary layer behaviour on continuous solid flat surfaces, Journal of AICHE, 7: 26-28.

[3] Crane, L. (1970). Flow past a stretching sheet. ZAMP, 21: 645-647.

[4] Chiam, T. C. (1994). Stagnation point flow towards a stretching plate. Journal of physical society of Japan, 63: 2443-2444.

[5] Andersson, K. I. Hansen, O. R. and Holmedal, B. (1994). Diffusion of a chemically reactive species from a stretching sheet. Int. Jr. Heat and Mass Transfer, 37: 659-664.

[6] Anjalidevi, S. P. and Kandasamy, R. (1999). Effect of chemical reaction, heat and mass transfer on laminar flow along a semi infinite horizontal plate convection in a porous medium. Heat Mass Transfer, Vol.28: 909-918.

[7] Muthucumaraswamy, R. (2002). Effects of chemical reaction on a moving isothermal vertical surface with suction. Acta Mech., 155: 65-70.

[8] Chamkha, A. J. Al-Mudhaf, A. and Al-Yatam, J. (2004). Double diffusive convective flow of a micro-polar fluid over a vertical plate embedded in a porous medium with a chemical reaction. Int. Jr. Fluid Mech. Res., 6: 529-551.

[9] Aboeldahab, E. M. and Azzam, G. E. A. (2006). Unsteady three dimensional combined heat and mass free convective flow over a stretching surface with time-dependent chemical reaction. Acta Mech., 184: 121-136.

[10] Tsai, R. and Huang, J. S. (2009). Heat and mass transfer for Soret and Dufour effects on Hiemenz flow through porous medium onto a stretching surface. Int. J. Heat Mass Transfer, 52 : 2399-2406.

[11] Rashad, A. M. and El-Kabeir, S. M. (2010). Heat and mass transfer in transient flow by mixed convection boundary layer over a stretching sheet embedded in a porous medium with chemically reactive species. Journal of Porous Media, 13(1): 75-85.

[12] Nayak, A., Panda, S. and Phukan, D. K. (2014). Soret and Dufour effect in a on mixed convection unsteady MHD boundary layer flow over stretching sheet in porous medium with chemically reactive species. Appl. Math. Mech.-Engl. Ed., 35(7): 849-862.

[13] Abbas, Z., Sheikh, M. and Pop, I. (2015). Stagnation point flow of a hydro-magnetic viscous fluid over a stretching/shrinking with generalized slip condition in the presence of homogeneous-heterogeneous reaction. Journal of the Taiwan Institute of chemical Engineers, 55: 69-75.

[14] Dash, G. C., Tripathy, R. S., Rashid, M. M. and Mishra, S. R. (2016). A numerical approach to boundary layer stagnation point flow past a stretching/ shrinking sheet. Journal of Molecular liquid, 221: 860-886.

[15] Seth, G. S., Singha, A. K., Mandal, M. ., Benerjee, A. and Bhattacharyya, K. (2017). MHD stagnation point flow and heat transfer past a non-isothermal shrinking/stretching sheet in porous medium with heat sink or source effect. International Journal of Mechanical Science, 134: 98-111.

[16] Veerkrishna, M., Gangadhara Reddy, M., and Chamkha, A. J. (2018). Heat and mass transfer on MHD free convective flow over an infinite non-conducting vertical porous plate, Int. J. Fluid Mech. Res., 45(5): 1-25.

[17] ShankarGoud, B. and Ganji, N. (2019). Stagnation point flow through a porous medium towards a stretching surface in the presence oh heat generation. International Journal of engineering and Advance Technology, 9(1): 2646-2650. https://doi.org/10.35940/ijeat.A.9880.109119

[18] Feleke, B. T., Oluwole, D. M. and Lemiguta, E. (2021). Stagnation flow of a magnetite ferro fluid past a convectively heated permeable stretching /shrinking sheet in a Darcy- Forchheimer porous medium. Sadhana (Indian Academy of Science), 46: 115. https://doi.org/10.1007/s12046-021-01643-46789

[19] Makinde, O. D., Borah, R. and Dey, D. (2022). Analysis of Dual Solutions in MHD Fluid Flow with Heat and Mass Transfer Past an Exponentially Shrinking/Stretching Surface in a Porous Medium. International Journal of Applied and Computational Mathematics, 8(article no.66).

[20] Vishalakshi, A. B., Mahabaleshwar, U. S., Parez, L. M. and Manca, O. (June 2023). Hiemenz stagnation point flow with computational modelling of variety of boundary conditions. Journal of Magnetism and Magnetic Materials, 575(1): 170747. https://doi.org/10.1016/j.jmmm.2023.170747

[21] Reddy, K. V. and Reddy, G. V. R. (2023). Outlining the impact modeling on MHD cassion fluid flow past a stretching sheet in a ,porous medium with radiation. Bioinferface Research in Apllied Chemistry, 13(1): 42. https://doi.org/10.33263/BRIAC131.042

[22] Kandagal, M. and Kampepatti, R. (2024). An investigation of the heat and mass transfer effects in vertical channels with immiscible fluid flow through a porous matrix, J. Appl. Math. Mech. (ZAMM), 104(10). https://doi.org/10.1002/zamm.202300998

[23] Sunitha, R. Y., Kalyan, K. P., Raghunath, K. and Farwa, A. (2024). Unsteady MHD rotating mixed convective flow through an infinite vertical plate subject to Joule heating, thermal radiation, Hall current, radiation absorption. Journal of Thermal Analysis and Calorimetry, 149: 8813-8826.

[24] Choudhary, S. and Choudhary, M. K. (2025). Heat and mass transfer by MHD flow near the stagnation point over a stretching or shrinking sheet in a porous medium. Indian Journal of Pure and Applied Physics, 54(3): 10681. https://doi.org/10.56042/ijpap.v54i3.10681

Biography

Deva Kanta Phukan is a former principal and professor at Demow College (Sivasagar), now retired. His research focuses on fluid dynamics and magnetohydrodynamics (MHD), contributing significantly to these fields during his academic career.